JGE (Jurnal Geofisika Eksplorasi)
Vol. 12 No. 01, March 2026 (73-91) https://doi.org/10.23960/jge.v12i1.512

BOUGUER ANOMALY AND SEDIMENT THICKNESS ESTIMATION AT THE TEHORU GEOTHERMAL AREA

ANOMALI BOUGUER DAN ESTIMASI KETEBALAN SEDIMEN DI KAWASAN PANAS BUMI TEHORU

Salman Hamja Siombone[1*], Mursaid Dahlan[2]

[1,2]Math Education Study Program, Department of Mathematics and Natural Sciences Education, STKIP Gotong Royong Masohi, District of Middle Moluccas, Moluccas Province, Indonesia

Received: 2026, March 05th
Accepted: 2026, June 01st

Keywords:
Bouguer Anomaly;
Reduced-Bouguer density;
Sediment Thickness;
Tehoru Geothermal Area;
TOPEX Gravity.

Corespondent Email:
salmansiombone@gmail.com

How to cite this article:
Siombone, S.H., & Dahlan, M. (2026). Bouguer Anomaly and Sediment Thickness Estimation at The Tehoru Geothermal Area. *JGE (Jurnal Geofisika Eksplorasi)*, 12(01), 73-91.

Abstract. Tehoru Village, Tehoru District, Central Maluku Regency, has significant geothermal potential. This study aims to examine Bouguer anomalies, reduced-Bouguer density, sediment thickness estimation, and shallow structures using TOPEX gravity data and SRTM DEM in an area of ±191.70 km². The processing results show Complete Bouguer Anomaly (CBA) values ranging from 6.80 to 73.60 mGal, with Bouguer densities of 1.77 to 1.79 g/cm³, indicating the dominance of alluvial sediments. Anomaly separation using the Moving Average method yields residual anomalies ranging from -4.60 to 47.70 mGal, with low anomalies dominant in the southwest of the geothermal manifestation. Spectral analysis shows an average sediment thickness of ±246.07 m. In contrast, SVD analysis, lineament maps, and rose diagrams indicate that geothermal manifestations develop in tight fault-related zones with a dominant northeast–southwest orientation. Although effective for regional analysis, TOPEX gravity data interpretation has limitations for imaging shallow structures and sediment thickness variations, as small anomalies are often obscured by its relatively low spatial resolution. Overall, the Tehoru geothermal system is controlled by several local fault-related zones and significant sediment thickness, which influence its response to tectonic activity.

Abstrak. *Desa Tehoru, Kecamatan Tehoru, Kabupaten Maluku Tengah, memiliki potensi panas bumi yang signifikan. Studi ini bertujuan untuk meneliti anomali Bouguer, densitas Bouguer tereduksi, estimasi ketebalan sedimen, dan struktur dangkal menggunakan data gravitasi TOPEX dan DEM SRTM di area seluas ±191,70 km². Hasil pengolahan menunjukkan nilai Anomali Bouguer Lengkap (CBA) berkisar antara 6,80 hingga 73,60 mGal, dengan densitas Bouguer 1,77 hingga 1,79 g/cm³, yang mengindikasikan dominasi sedimen aluvial. Pemisahan anomali menggunakan metode Rata-Rata Bergerak menghasilkan anomali residual berkisar antara -4,60 hingga 47,70 mGal, dengan anomali rendah dominan di barat daya manifestasi panas bumi. Analisis spektral menunjukkan ketebalan sedimen rata-rata ±246,07 m. Sebaliknya, analisis SVD, peta lineamen, dan diagram mawar menunjukkan bahwa manifestasi panas*

bumi berkembang di zona-zona yang berdekatan dengan sesar dengan orientasi dominan timur laut–barat daya. Meskipun efektif untuk analisis regional, interpretasi data gravitasi TOPEX memiliki keterbatasan untuk pencitraan struktur dangkal dan variasi ketebalan sedimen, karena anomali kecil seringkali tersembunyi oleh resolusi spasialnya yang relatif rendah. Secara keseluruhan, sistem panas bumi Tehoru dikendalikan oleh beberapa zona lokal yang berdekatan dengan sesar dan ketebalan sedimen yang signifikan, yang memengaruhi responsnya terhadap aktivitas tektonik.

1. INTRODUCTION

Tehoru, located in Central Maluku Regency, is one of the geothermal prospect areas in Seram Island, characterized by surface manifestations such as hot springs, hydrothermal alteration, and steaming ground. Previous studies reported that the hot springs in this area have surface temperatures ranging from 74°C to 97°C (Siombone, 2022; Siombone et al., 2024). Unlike volcanic geothermal systems directly associated with active volcanism, the Tehoru geothermal manifestations are interpreted to be strongly influenced by the tectonic setting of Seram Island, which lies within the active Banda Arc region and is affected by the interaction of the Eurasian, Indo-Australian, and Pacific plates (Hill, 2012; Sapiie & Hadiana, 2013; Daniarsyad et al., 2023).

The geothermal system in Tehoru is closely related to local geological structures, particularly faults and fractures that act as permeability pathways for geothermal fluid migration. In the Telutih–Tehoru area, tectonic deformation is associated with the Kawa Fault system, including the Telutih Segment, which contributes to local seismic activity and structural complexity (Daniarsyad et al., 2023). The occurrence of the 2019 Ambon earthquake and the 2021 Tehoru earthquake further indicates that this region is tectonically active (Pelupessy & Silverman, 2024). Therefore, identifying shallow structures, weak zones, and density variations is important for understanding the geological controls of the Tehoru geothermal system and its relationship with local tectonic activity.

Several previous studies in the Tehoru geothermal area have focused on surface characteristics, including Landsat 8 imagery, geothermal fluid geochemistry, and alteration rock petrography (Andayany & Risakotta, 2017; Toisuta et al., 2021; Siombone, 2022). These studies provided important information on surface temperature distribution, geomorphology, fluid chemistry, reservoir temperature estimation, and alteration minerals. However, gravity-based analysis using satellite-derived data has not been specifically applied to evaluate Bouguer anomalies, near-surface density, sediment thickness, and shallow structural patterns in the Tehoru geothermal area. This creates a research gap, particularly in understanding whether the geothermal system is dominantly controlled by tectonic processes rather than volcanic activity.

Direct field gravity acquisition in the Tehoru area is constrained by steep topography, valleys, and limited accessibility. Therefore, TOPEX satellite gravity data integrated with SRTM DEM provide an effective preliminary approach for regional-scale subsurface interpretation. TOPEX gravity data can be used to analyze Bouguer anomalies, density contrast, residual anomalies, and sediment thickness, while SRTM DEM supports topographic and lineament interpretation. Although TOPEX data have lower spatial resolution than field gravity surveys, they remain useful for preliminary geothermal and tectonic studies, especially in areas where direct measurements are limited.

Based on these considerations, this study aims to identify the subsurface characteristics of the Tehoru geothermal area using TOPEX gravity data and SRTM DEM. The analysis focuses on Complete Bouguer Anomaly, reduced-Bouguer density, regional–residual anomaly separation, sediment thickness

estimation, and Second Vertical Derivative (SVD) interpretation. The results are expected to clarify the relationship between gravity anomaly patterns, shallow structural controls, sediment thickness, and geothermal manifestations in the Tehoru area.

2. LITERATURE REVIEW

2.1. Location of the Study Area

The study area for this research covers the geothermal area of Tehoru village, the coastal area, the sea area of Tehoru village (around Telutih Bay), part of the Haya village area, and the area around the epicenter of the 2021 earthquake. The Tehoru geothermal area in Central Maluku Regency is one of the areas with geothermal prospects characterized by the manifestation of hot springs, with geological conditions including undulating geomorphological features and a close structural lineament (Siombone, 2022; Toisuta et al., 2021). This study area encompasses 56 TOPEX gravity acquisition points, covering a total area of 191.70 km², with a spacing of ±1.85 km between them. The location map of the study area is shown in **Figure 1**.

Based on **Figure 1**, 56 TOPEX gravity acquisition points are spread across the study area: 34 are located in land areas and 22 in marine areas. The majority of gravity acquisition points in this study area were located on land to map and assess the pattern and continuity of gravity anomalies around the Tehoru geothermal area. Several TOPEX gravity acquisition points were taken in the marine area to allow the authors to observe gravity anomalies spread across the coastal and marine areas of the Tehoru village geothermal area.

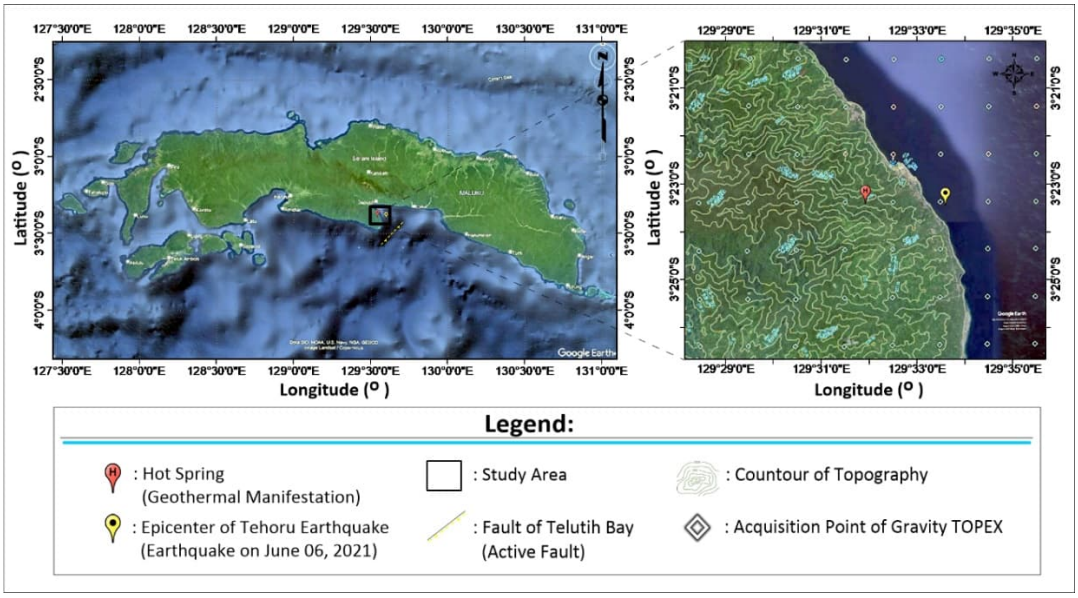

Figure 1. Location of the Study Area.

2.2. Local Geological Setting of The Study Area

Stratigraphically, Seram Island consists of metamorphic, sedimentary, intrusive, and tectonic rocks (Tjokrosapoetro et al., 1993). The oldest rocks that make up the bedrock of Seram Island are the Taunusa and Tehoru Complexes, which are Permian in age and are overlain by alluvial deposits, the youngest units in this area. The bedrock of Seram Island consists of high-grade to low-grade metamorphic rocks from the Kobipoto Complex, Taunusa, Tehoru, and Saku formations. These three metamorphic complexes were exposed at the surface due to thrust faulting during the Late Miocene and Pliocene and then experienced strike-slip faulting. The oldest sedimentary rocks on Seram Island are the Kanikeh Formation, deposited in the outer neritic zone and

consisting of sandstone and mudstone, and unconformably overlies metamorphic rocks. The Kanikeh Formation is Middle Triassic-Late Triassic in age. Above the Kanikeh Formation, gradationally, is the Saman-Saman Formation, which consists of limestone. Then, directly above the Saman-Saman Formation, there is the Manusela Formation, which consists of limestone and was deposited in a neritic-bathyal environment (Samalehu et al., 2024; Sapiie & Hadiana, 2013). The general regional stratigraphic and geological conditions on Seram Island have been described. Meanwhile, the local geological conditions of the Tehoru geothermal area can be seen on the geological map in **Figure 2**.

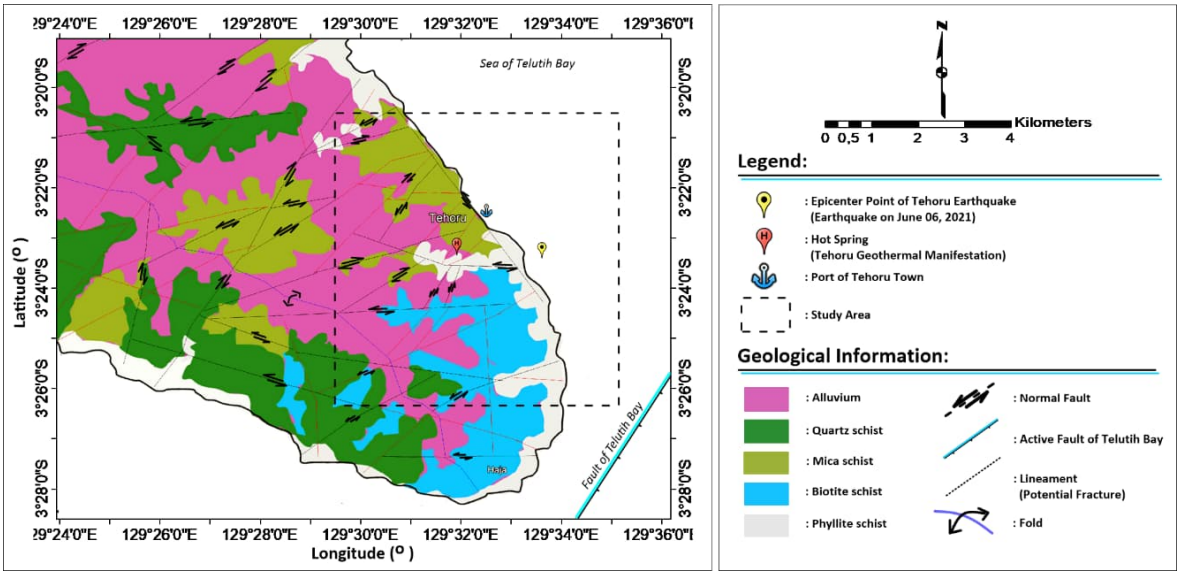

Figure 2. Geological setting of the study area, modified from Directorate of Geothermal Energy (2017).

2.3. Gravity Method, TOPEX Data, Sediment Thickness and SVD

The gravity method is a geophysical technique used to identify subsurface geological conditions based on variations in the Earth's gravitational field caused by differences in rock density. In geothermal studies, gravity data are useful for delineating density contrasts, structural lineaments, fault zones, sedimentary basins, and possible subsurface controls of fluid circulation. Therefore, this method is relevant for interpreting the geological framework of the Tehoru geothermal area, particularly in relation to fault-controlled geothermal manifestations and shallow sediment distribution.

In this study, TOPEX satellite gravity data were used as the main gravity dataset because they provide open-access gravity anomaly information and allow regional-scale interpretation, especially in areas where direct field acquisition is constrained by steep topography and limited accessibility. TOPEX gravity data have been widely applied for regional tectonic, marine, and geothermal studies. However, their spatial resolution is lower than field gravity surveys, so small-scale anomalies and shallow structures may be smoothed or less clearly resolved. For this reason, TOPEX-based interpretation should be regarded as a preliminary regional analysis and ideally validated with field gravity or other geophysical data.

Sediment thickness was estimated using spectral analysis of Bouguer anomaly data. This approach separates regional and residual anomaly components based on their frequency characteristics, where long-wavelength anomalies generally represent deeper sources and short-wavelength anomalies are associated with shallower geological features. In geothermal and tectonically active areas, sediment thickness information is important

because it may reflect basin geometry, shallow structural controls, and zones that can influence seismic-wave amplification.

The Second Vertical Derivative (SVD) method was applied to enhance shallow gravity anomaly responses and clarify lateral density contrasts. SVD is useful for identifying geological boundaries such as faults, fractures, lithological contacts, and basin margins. In this study, SVD analysis was integrated with Bouguer anomaly interpretation, sediment thickness estimation, and lineament analysis to evaluate the relationship between shallow structures and geothermal manifestations in the Tehoru area.

3. RESEARCH METHODS

3.1. Material

The materials referred to in this research include the data and the tools (software) used to acquire and process them. The data used in this research include TOPEX satellite gravity/elevation data, and SRTM Digital Elevation Model (DEM) imagery. This TOPEX satellite data was obtained via the page https://topex.ucsd.edu/cgi-bin/get_data.cgi. This Topex gravity data was downloaded on December 25, 2025. Meanwhile, the DEM SRTM data was obtained via the page: https://earthexplorer.usgs.gov/. This SRTM DEM data was downloaded on November 10, 2024. The TOPEX gravity data is a high-resolution global ocean gravity anomaly dataset, typically on a 1-minute grid, derived from satellite altimetry (such as Jason-1, CryoSat-2, Geosat, ERS-1) and shipboard surveys (Sandwell et al., 2014). This data is used to map seafloor topography, tectonic structures, and free-air gravity anomalies (Siombone et al., 2022). Meanwhile, the Shuttle Radar Topography Mission (SRTM) DEM is a radar-based digital elevation model produced by NASA, covering nearly 80% of Earth's surface with spatial resolutions of 30 meters or 90 meters (Siombone et al., 2022; USGS, 2016). This data is crucial for topographic mapping, hydrological analysis, and global geospatial studies. Several applications were used in this research, including the Ms. Excel v.19, the Global Mapper app v.19, the Suffer 16 App, the Dips 7.0, the ArcGIS V.18 App, and MATLAB V.21. The gravity data and surface-marine topography obtained from the TOPEX page are still in free-air gravity anomaly and elevation data form. Hence, they need to be corrected for several gravity effects to obtain gravity anomalies at the research location. The SRTM DEM data is needed and used during the gravity correction process (i.e., the Terrain correction), making topographic elevation maps, lineament maps (ridge-and-valley lineament), and Rose diagrams of lineament orientation patterns.

3.2. Method

The downloaded TOPEX gravity data is still in the form of free-air gravity anomalies, with topographic data from the SRTM DEM, which will be processed through a series of gravity corrections to obtain Bouguer anomaly data. Simple Bouguer anomaly data and complete Bouguer anomaly data can be obtained through the following equation:

$$\mathrm{FAA} = (g_{obs} - g_{\varphi}) + \Delta g_{FA} \quad (4)$$

$$\Delta g_{SBA} = \mathrm{FAA} - \Delta g_{B} \quad (5)$$

$$\Delta g_{CBA} = \Delta g_{SBA} + \Delta g_{T} \quad (6)$$

where FAA is the Free Air Anomaly gravity value (mGal), g_{obs} is the observed gravity value (mGal), g_{φ} is the latitude gravity value (theoretical correction) (mGal), Δg_{FA} is the free air correction (mGal), Δg_{B} is the Bouguer Correction (mGal), and Δg_{T} is the terrain correction (mGal). While Δg_{SBA} is the simple Bouguer anomaly (mGal), and is the Δg_{CBA} complete Bouguer anomaly.

The existing gravity anomaly data, in the form of FAA values, Δg_{B} values, and Δg_{T} values, can also be used to determine the average near-surface rock (reduced-Bouguer density) for the study area. The reduced-Bouguer density will be determined using two methods: the Parasnis and Nettleton methods. The next step, using complete Bouguer anomaly data, will be to separate regional and residual anomalies using the Moving Average (MVA) method. The moving-average process

is performed during the spectrum analysis stage of the digitized gravity data using the Fast Fourier Transform (FFT) (Wahyudi et al., 2019). The digitized gravity data along each path (slice) will be converted to the frequency domain using the FFT (Siombone et al., 2022). Blakely (1996) derived the spectrum of the observed potential gravity force on a horizontal plane, namely:

$$F(\mathrm{U}) = G\rho\, F\left(\frac{1}{r}\right) \quad (7)$$

$$F\left(\frac{1}{r}\right) = 2\pi \frac{e^{k(z_0 - z')}}{|k|} \quad (8)$$

Based on the two equations above, we obtain:

$$F(\mathrm{U}) = 2\pi\lambda\rho \frac{e^{k(z_0 - z')}}{|k|} \quad (9)$$

So the Fourier transform (FFT) of the gravity anomaly on the desired trajectory is:

$$F(\mathrm{g}_z) = G\rho\, F\left(\frac{\partial 1}{\partial z\, r}\right) \quad (10)$$

$$F(\mathrm{g}_z) = G\rho \frac{\partial}{\partial z} F\left(\frac{1}{r}\right) \quad (11)$$

$$F(\mathrm{g}_z) = 2\pi G\rho\, e^{k(z_0 - z')}\,;\, z' > z_0 \quad (12)$$

If the density distribution is random and there is no correlation between each value of the gravitational acceleration g_z, then $\rho = 1$, so that the result of the Fourier transform (FFT) of the gravity anomaly is (Sarkowi, 2014):

$$\mathrm{A} = \mathrm{C}\, e^{k(z_0 - z')} \quad (13)$$

Next, by logarithmizing the FFT results above, the relationship between amplitude (A), wave number (k), and depth $(z_0 - z')$ will be obtained as:

$$\ln A = (z_0 - z')|k| \quad (14)$$

Where, U is the gravitational potential (m^2/s^2), ρ is the mass density anomaly (gram/cm^3), G is the universal gravitational constant (N m^2 kg^{-2}); r is the distance to the center of the anomaly (meters); g_z is the vertical component of the gravitational anomaly (mGal), A is the amplitude (mGal); k is the wave number (m^{-1}), z_0 is the observation point (m), and z is the depth of the anomalous object (m).

After the spectrum analysis is carried out, window width [N] data set will be obtained, which is used to separate regional and residual anomalies, and, by utilizing the MVA filter, regional Bouguer anomaly data will be obtained. The window width used to separate regional and residual anomalies from the Complete Bouguer Anomaly (CBA) is a filtering parameter that determines the size of the data area used in the smoothing process. Larger N values produce stronger smoothing, allowing low-frequency components or regional anomalies to dominate, while local/shallow anomalies tend to be reduced (Abdelrahman & El-Araby, 1996; Ramadhan & Pohan, 2024; Wahyudi et al., 2019). Conversely, smaller N values retain high-frequency components, making residual anomalies more visible. The next stage can be carried out during the separation of the regional Bouguer anomaly and the residual Bouguer anomaly from the complete Bouguer anomaly. Regional Bouguer anomaly data and residual Bouguer anomaly will then be used for qualitative interpretation of deep subsurface structures (e.g., basement) and shallow subsurface structures (e.g., sediment thickness). Analysis of shallow-depth data (residual anomalies) will be displayed in a 3D model of sediment thickness for the study area. Using the Bouguer Anomaly data obtained, the process of determining the second vertical derivative (SVD) anomaly is carried out. The SVD anomaly can be used to interpret the shallowest structures, such as fault lines, lineaments, or geological contact boundaries (Blakely, 1996). To determine the SVD anomaly, the Fourier transform is applied in the wave domain. The Fourier transform operator used in the SVD method is the 5×5 Elkins matrix of order 5 (See **Table 1**). Overall, the relationship between TOPEX data and DEM-SRTM data is integrated into a systematic methodological framework, as represented in the Research Workflow Diagram in **Figure 3**.

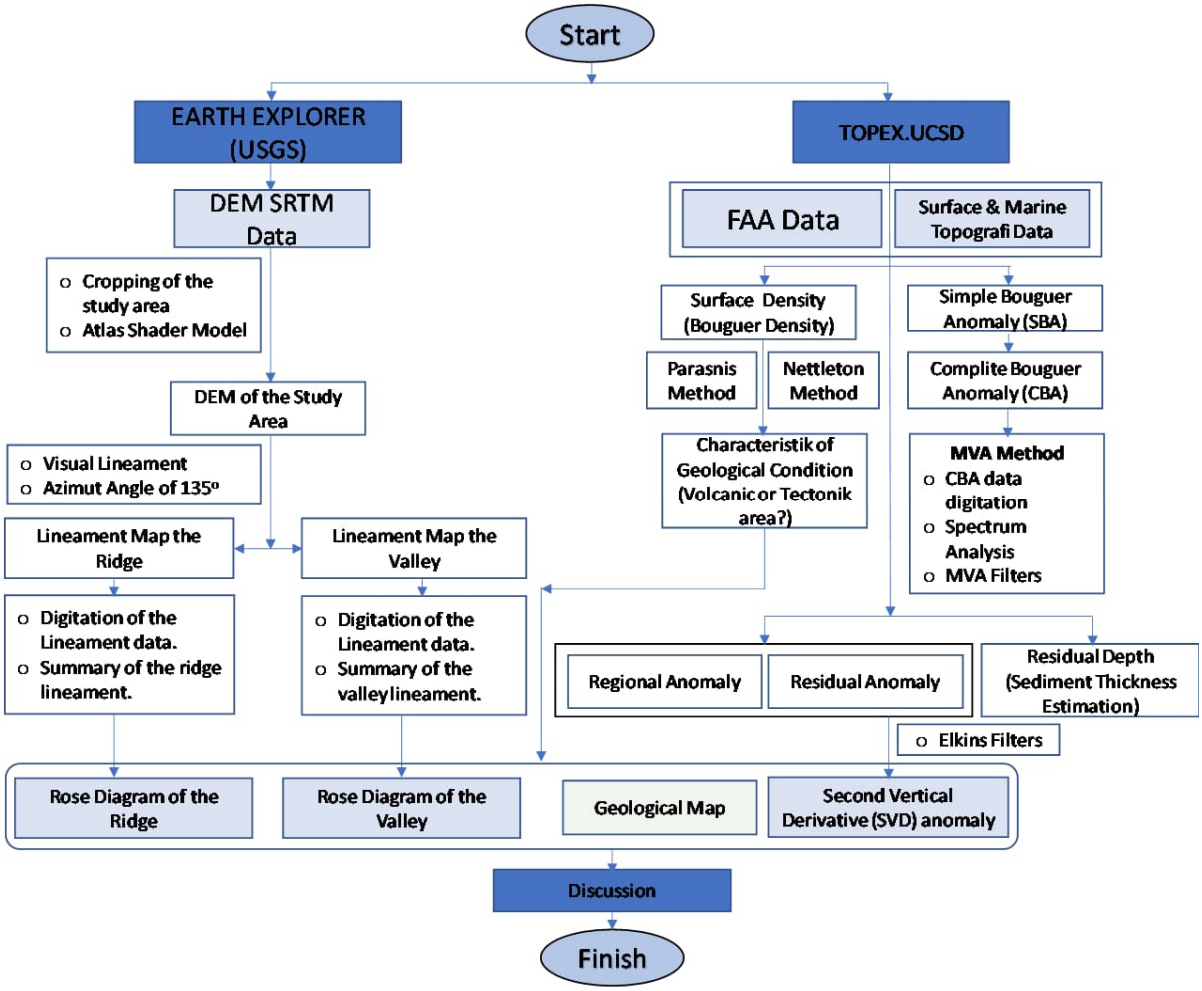

Figure 3. Research Workflow Diagram.

4. RESULTS AND DISCUSSION

The research results will be discussed in stages, starting with simple Bouguer anomaly data, complete Bouguer anomaly, determination of Bouguer density, spectrum analysis for separation of regional and residual anomalies, interpretation of regional and residual anomalies, sediment depth modeling, and interpretation of second vertical derivative (SVD) anomalies.

4.1. Complete Bouguer Anomaly and Reduced-Bouguer Density

The Complete Bouguer Anomaly (CBA) in the Tehoru geothermal area ranges from 6.80 to 73.60 mGal (**Figure 4)**. Low Bouguer anomalies are mainly distributed in the western part of the study area and form a northwest–southeast trend, whereas high anomalies are more dominant toward the eastern and northern parts. The geothermal manifestation is located near the boundary between low and moderate Bouguer anomalies, suggesting a lateral density contrast that may be associated with fault-related permeability zones and lithological variation.

Reduced-Bouguer density estimation using the Parasnis and Nettleton methods yields consistent values of 1.77–1.79 g/cm^3. The Parasnis method gives a density of 1.792 g/cm^3, whereas the Nettleton method gives an average value of 1.77 g/cm^3. These relatively low density values indicate that the near-surface materials are dominated by unconsolidated to weakly consolidated alluvial sediments. In relation to the local geological setting, this condition supports the interpretation that the Tehoru geothermal system is structurally controlled rather than directly associated with volcanic rocks.

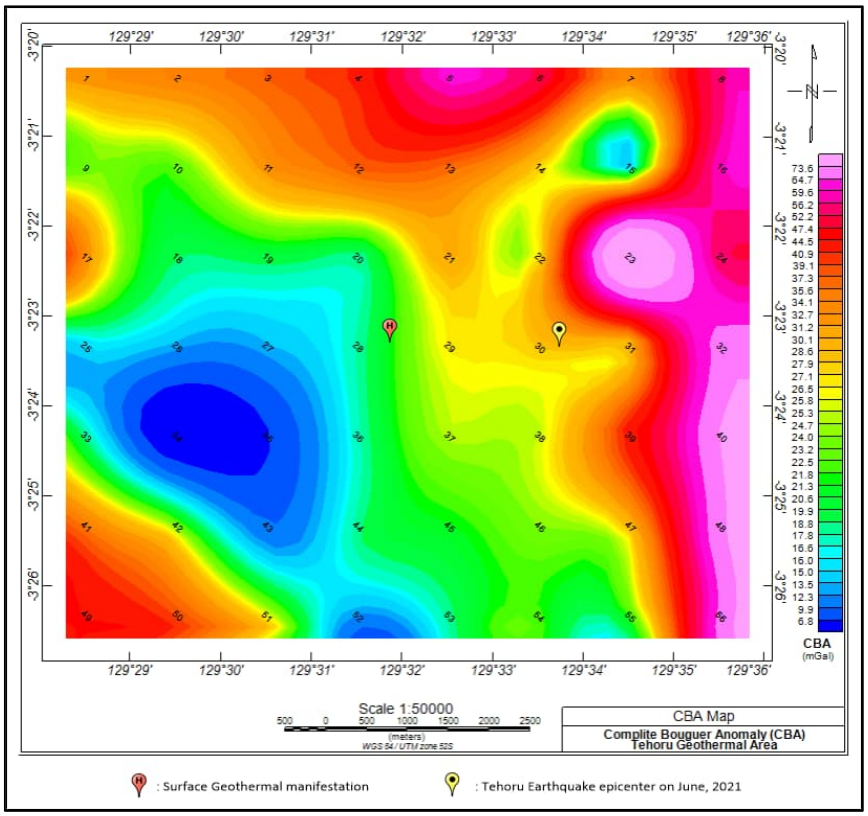

Figure 4. Complete Bouguer Anomaly distribution map.

4.1.1. Parasnis Method

The Parasnis method is a statistical method for estimating the best reduced-Bouguer density from gravity data and elevation. This method determines the rock density that best matches local geological conditions. This method can be performed by analyzing the linear relationship (regression) between free-air anomalies (FAA) and elevation (Bouguer Correction minus terrain correction) (Siombone et al., 2022). The slope of the regression line is used to calculate the optimum reduced-Bouguer density (Sarkowi, 2014). The reduced-Bouguer density Estimation graphic display is shown in **Figure 5.**

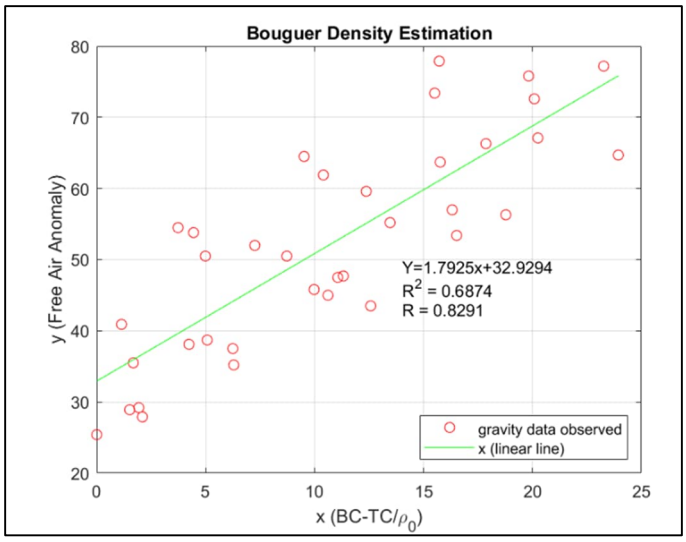

Figure 5. Reduced-Bouguer Density of the Study Area.

Figure 5 shows an estimated Reduced Bouguer density of 1.792 g/cm³ for the study area, with a coefficient of determination (R^2) of 0.687. This result indicates that the regression model accounts for approximately 68.70% of the variability in the observed data, reflecting a moderate-to-strong linear relationship between the variables analyzed. The relatively low density, when considered together with the regional geological setting, suggests that the near-surface subsurface is dominated by unconsolidated to weakly consolidated alluvial sedimentary deposits

4.1.2. Nettleton Method

The Nettleton method is based on the understanding of Bouguer correction and terrain correction, where if the mass density used matches the surface density, the gravity anomaly cross-section or profile becomes "smooth." The Bouguer anomaly at a point along a trajectory is plotted for various values of mass density (ρ). The surface density is determined if the resulting gravity anomaly does not correlate with the topography in the area (Nettleton, 1939; Sarkowi, 2014). The Nettleton method determines reduced-Bouguer density by selecting a density value that makes the Bouguer anomaly uncorrelated with topography (Gunawan & Mikhailov, 2008). Density is calculated for several experimental values, then the one that produces the smoothest Bouguer anomaly curve and is independent of surface relief (hill-valley) is selected. This value is considered the average density of the surface rocks in the study area. The estimated reduced-Bouguer density value of the study area is shown in **Figure 6**.

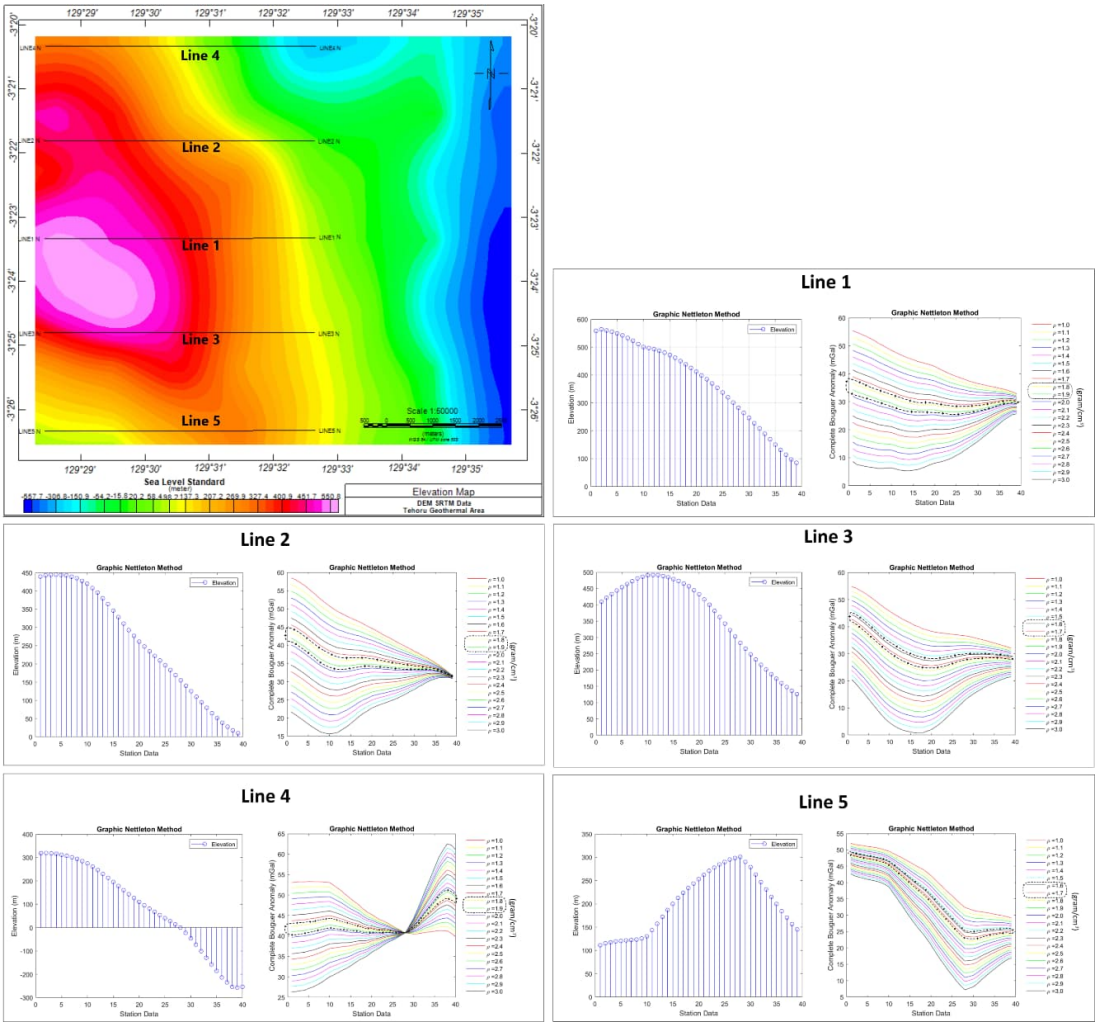

Figure 6. Estimation of reduced-Bouguer density in the study area using the Nettleton method.

The digitization results for five line slices with a data spacing of 200 meters for FAA anomaly data, Elevation data, and Terrain correction data were then plotted. Referring to **Figure 6** above lineslice-1 has ρ_1 is 1.85 g/cm^3, lineslice-2 has ρ_2 is 1.85 g/cm^3, lineslice-3 has ρ_3 is 1,65 g/cm^3, lineslice-4 has ρ_4 is 1,85 g/cm^3, and lineslice-5 has ρ_5 is 1,65 g/cm^3. Based on the digitization results from the five line slices surrounding the geothermal area, the mean density across these slices was adopted as the representative average surface density. Consequently, the estimated reduced-Bouguer density ($\rho_{Average}$) for the Tehoru geothermal area was determined to be 1.77 g/cm^3. The average Bouguer density value above was chosen because it is the least correlated with local topography (Nettleton, 1939). This density value is consistent with geological information indicating that the geothermal area of Terhoru village is dominated by alluvial deposits characteristic of the coastal area, with several river estuaries that correlate with straight lines and small faults.

Based on reduced-Bouguer density estimates obtained using the Parasnis Method and the Nettleton Method, a consistent correlation in the reduced-Bouguer density (ρAverage) range of 1,77–1,79 g/cm^3 was identified across the study area. When considered in relation to the local geological conditions of the Tehoru geothermal area, this density value indicates the dominance of alluvial sedimentary lithology, characterized by loose, poorly consolidated materials, compared to other rock units within the local geological formation. The relatively low rock density further confirms that the lithological units composing the Tehoru geothermal research area are products of tectonic activity rather than volcanic processes. Previous studies conducted by Toisuta et al. (2021) using geochemical methods revealed that all hot spring manifestations were characterized by bicarbonate-type waters (peripheral waters) with elevated Cl content influenced by seawater contamination. These characteristics indicate the mixing of hydrothermal fluids with meteoric water within the peripheral zone of a geothermal system controlled by faults and fracture structures. Furthermore Andayany & Risakotta, (2017) identified, through petrographic analysis, the dominance of microcrystalline calcite particles, which are commonly associated with fault-controlled geothermal systems. This mineral generally forms by precipitation of carbonate-rich hydrothermal fluids along fractures, faults, and permeable zones, driven by changes in temperature, pressure, and CO_2 degassing.

The relatively low density indicates that the study area is tectonic rather than volcanic. This condition is associated with high-intensity fault structures, where fractures increase rock porosity and permeability, thereby facilitating the migration of geothermal fluids from the subsurface reservoir to the surface. Geologically, young rock units in the Tehoru area are also dominated by alluvial deposits resulting from river estuary sedimentation, especially those originating from the Yapana River, which triggers the accumulation of quite thick sediments along the coastal zone.

4.2. Separation of Regional and Residual Anomalies

The process of separating regional and residual Bouguer anomalies from the complete Bouguer anomaly (CBA) in this study used the Moving Average method. During the implementation of this Moving Average method, a digitization process was carried out on 9 data lines slice the complete Bouguer anomaly map, as shown in **Figure 7.** In the data digitization process, a distance of 200 meters was required between each line (slice) of gravity data on the CBA map. The digitised gravity data from the CBA map will be processed using a Fourier transform to produce 1-D FFT input data. This 1-D FFT gravity data essentially represents information (signals) related to gravity values in the vertical component g_z, and is commonly used to determine depth information on subsurface anomalous bodies. The FFT calculation on each gravity data requires 2^n for each line slice. The 1-D gravity data resulting from the FFT is

then processed and plotted in a graph showing the relationship between the wave number (k) and the logarithm of the Amplitude (ln A). The graph of the relationship between k and ln A is shown in **Figure 7**.

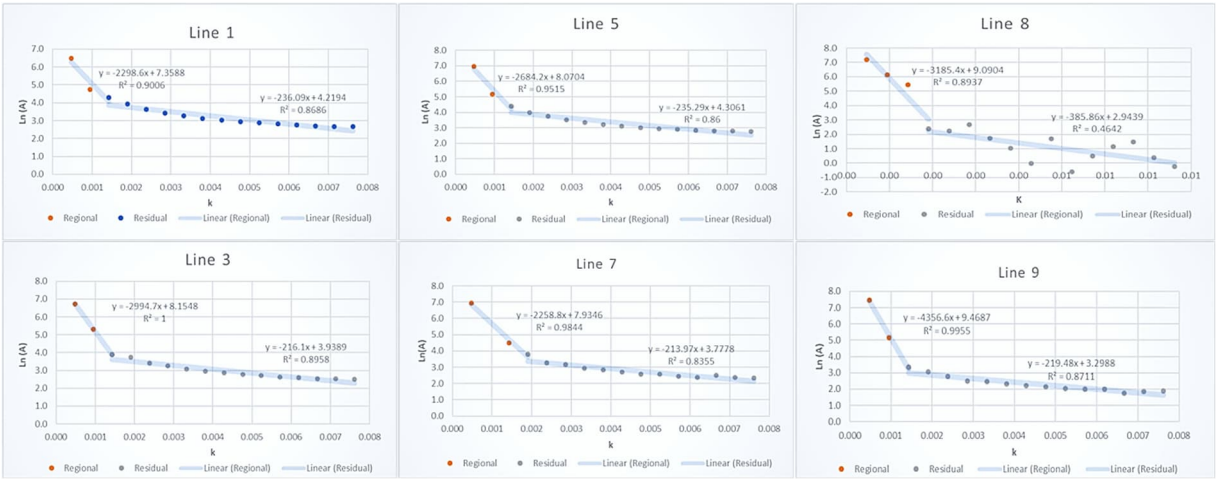

Figure 7. Graph of the power spectrum of each line.

The power spectrum graph shown in **Figure 7** provides information on the depth of the residual (sedimentary) anomaly source and the regional (basement) anomaly source. Based on the depth of regional and residual anomaly sources, calculations can be performed to obtain the wave number (k-cutoff) and window width (N). The equation used in determining the wave number is given by equation (15) and (16) below (Siombone et al., 2022; Wahyudi et al., 2019):

$$N = \frac{\lambda}{\Delta x}, \text{ with } \lambda = \frac{2\pi}{k_{cutoff}}, \text{ so that;} \quad (15)$$

$$N = \frac{2\pi}{k_{cutoff}} \cdot \frac{1}{\Delta x} = \frac{2\pi}{k_{cutoff} \cdot \Delta x} \quad (16)$$

In the Bouguer anomaly power spectrum study, the wavenumber k cut-off is the wavenumber limit value used to separate the regional and residual gravity anomaly components based on the depth of the anomaly source. Meanwhile, in the CBA data power spectrum study, the window width (N) is the size of the data's spatial domain (path length or area) used during spectral analysis to determine the boundary between regional and residual anomalies objectively.

Some *k-cutoff* values were derived from the power spectrum analysis and substituted into Equation (7), resulting in a window width of N = 19. The calculated value (N = 19.364) was rounded to 19 following standard mathematical rounding rules, as the filtering process requires the window width to be expressed as an integer. The single-window width data and a 5x5 symmetric convolution matrix (a moving-average filter) are used to detect regional anomalies from the CBA data. The filtering process for the CBA data produces regional anomalies.

Furthermore, by utilizing CBA data and regional anomaly data through the following equation (10), the residual anomaly data can be determined. Equation 8 is given by:

$$\Delta g_{res} = \Delta g_{CBA} - \Delta g_{reg} \quad (17)$$

where Δg_{res} is the residual anomaly data, Δg_{CBA} is the complete Bouguer anomaly data, and Δg_{reg} is the regional anomaly data.

4.3. Regional and Residual Bouguer Anomaly

Regional anomalies are essentially components of gravity anomalies that represent the influence of large-scale, deep-seated mass sources, derived from the CBA data after the local (residual) components have been removed or smoothed. These anomalies reflect the regional gravity trend of an area or the general geological conditions and provide information regarding the structure of the

basement layer (Siombone et al., 2022). The display of regional anomalies after filtering using the moving-average method.

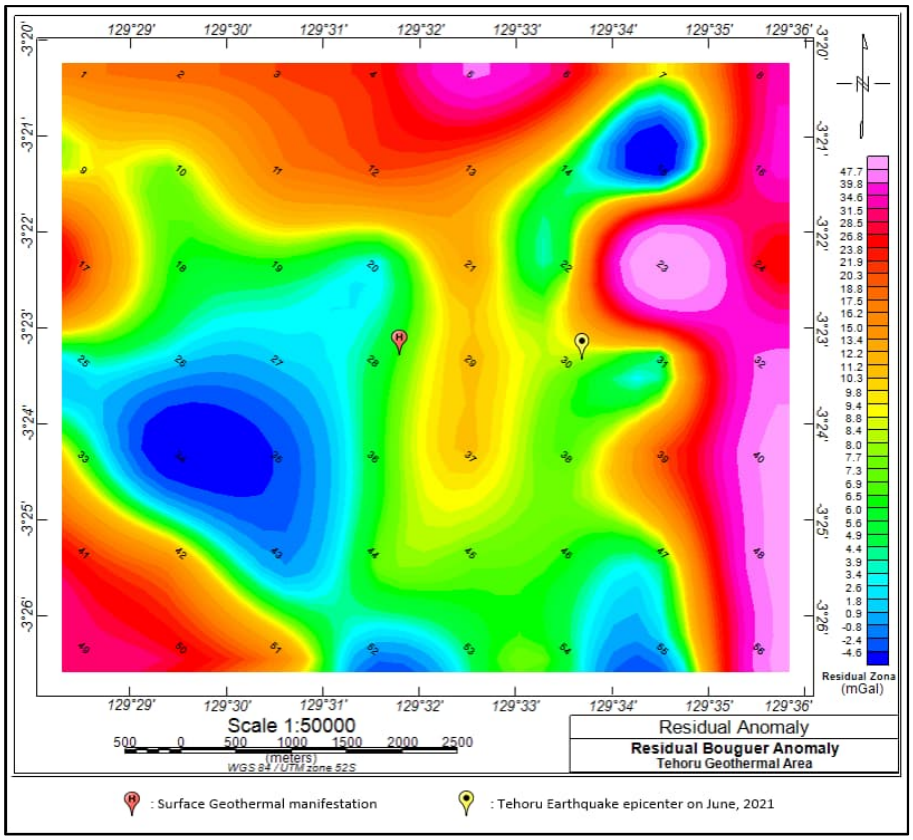

Figure 8. Residual Bouguer map of the study area.

Based on the residual anomaly data as shown in **Figure 8** above, the residual Bouguer anomaly in the study area ranges from -4.60 mGal to 47.70 mGal. Based on the residual anomaly data on the map, the low-anomaly range is -4.60 to 2.90 mGal. This low residual anomaly is located in the west of the study area, with a small portion in the south, southeast, and northeast. This low residual anomaly is located southwest of the geothermal manifestation (hot springs) on the edge of the Yapana River Basin. This low residual anomaly is parallel to the moderate anomaly around the geothermal manifestation, forming a northwest-southeast trend. This result is in line with the research of Prasetyo et al. (2025) who found that geothermal manifestations are located in the fault zone, which is the boundary between the high- and low-anomaly areas. One indication of a geothermal system is the presence of geothermal manifestations on the Earth's surface, such as hot springs, steaming soil, warm water, and mud pools. These geothermal manifestations typically appear around weak zones or fault systems (Prasetyo et al., 2025). Furthermore, low gravity anomalies typically indicate substantial sediment deposition. These zones typically have lower density than the surrounding rocks (Prasetyo et al., 2025).

4.4. Sediment Depth

The residual Bouguer anomaly depth is assumed to represent sediment thickness because it reflects a shallow mass source with a low density contrast, which is generally associated with sediment layers above bedrock (Dewanto et al., 2023; Segoro & Margiono, 2025). After the regional component is separated, the residual anomaly's variation is

dominated by changes in sediment thickness. The sediment thickness estimation in this study was carried out using a power spectrum analysis of the Complete Bouguer Anomaly (CBA) data via a 1D FFT, as shown in Figure 9 (Peng et al., 2025). Spectrum analysis allows identification of the source depths of regional and residual anomalies, with the residual depth projected as sediment thickness.

This residual anomaly depth data is then projected into a sediment thickness model as shown in **Figures 9a** and **Figure 9b**. The use of residual gravity anomalies as a preliminary indicator of sediment thickness is supported by numerous previous studies (Abdullahi, 2022; Dewanto et al., 2023; Prabowo et al., 2022), and has been further applied in more recent investigations (Armi, 2025; Segoro & Margiono, 2025; Sfada & Ali, 2025). Several previous studies above utilize residual anomaly depth data to describe sediment thickness in a study area, with residual depths varying depending on the focus or target of the interpretation being investigated, whether the study is a local or regional area review.

Based on **Figure 13a**, there are nine line slices from line A-A' to line I-I' on the body of the CBA map. These nine line slices are oriented west to east. Where seven line slices are above sea level, namely lines A-A' to G-G', while two line slices, lines H-H' and I-I', are below sea level, precisely in the Telutih Bay area. The depth data from each residual anomaly source on all existing line slices ranges from -213.97 m to -385.86 m below sea level, with an average depth of -244.90 m below sea level. The depth of this residual anomaly describes the thickness of sediment in the study area (Prabowo et al., 2022; Segoro & Margiono, 2025). Referring to the 3D modeling data for all line sections in **Figure 9a**, the greatest sediment thickness is at the H-H' line section, with a thickness of 385.86 m, located on the seabed at a depth of -103.429 m. The line with the greatest sediment thickness, as shown on the study area map, is located in the Telutih Bay sea area, east of the Tehoru village coast (see **Figure 1**).

Based on **Figure 9b**, eight north–south oriented line slices, from J–J' to Q–Q', were created on the Complete Bouguer Anomaly (CBA) map. Modeling shows that the depth of the residual anomaly source ranges from −194.64 m to −323.71 m below sea level, with an average of −247.24 m. This depth can be interpreted as sediment thickness because it lies well above the regional bedrock (Dewanto et al., 2023). The 3D modeling results indicate that the maximum sediment thickness is located at the O–O' line at 323.71 m, in the southern part of the Tehoru geothermal prospect. This zone is thought to be related to rock alteration and weathering processes, driven by geothermal activity and the presence of fault structures or fractures around the geothermal manifestations. In addition, alluvial deposits from the Yapana River basin are thought to fill the fracture zone in this fault system. Therefore, the depth of the residual anomaly physically and geologically represents the depth and thickness of the sedimentary layer. 3D modeling results indicate an average sediment thickness of 246.07 m, which may contribute to seismic wave amplification and the level of damage caused by tectonic earthquakes, particularly in loose to semi-consolidated sediments (Dewanto et al., 2023; Maringue et al., 2021). Geophysically, this thickness is considered significant for site effects.

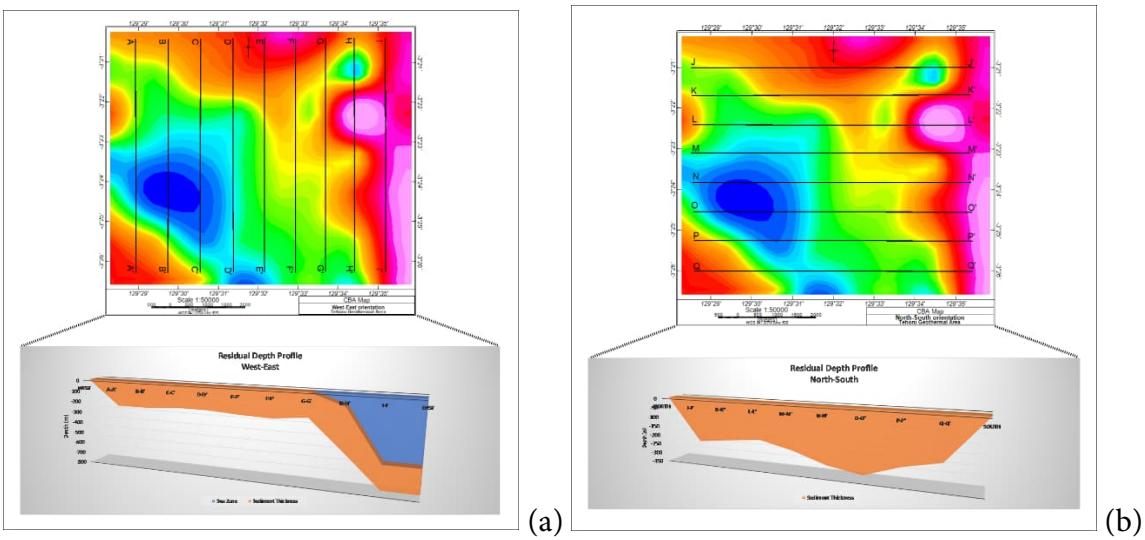

Figure 9. (a) Sediment thickness profile of each line slice with West-East orientation and (b) North-South orientation.

Referring to the west-east- and north-south-trending residual depth profiles in **Figures 9a** and **Figure 9b**, the sediment thickness characteristics in the Tehoru geothermal area show similarities with several previous studies of tectonic and volcanic-tectonic (volcanogenic) systems. Research by Sismanto et al. (2022) applied field data from the Kadidia geothermal field, Central Sulawesi, using gravity data and spectral analysis, yielding residual anomalous depths of around −80 to −150 m, indicating relatively shallow sediment thickness. Meanwhile Rasimeng et al. (2024), using GGMPlus data in the Wayratai geothermal area, Lampung, which developed in a volcanogenic environment, obtained residual anomalous depths ranging from −286.49 to −351.29 m, with an average of −321.93 m, which are similar to the sedimentation profile in Tehoru. Research by (Dewanto et al. (2023) using and applying GGMPlus data in the Majene tectonic area, West Sulawesi, reported sediment thickness ranging from −302.57 to −1109.2 m, while (Zakariah et al. (2021) in the Muda River Basin, Malaysia, using and applying field data, obtained a shallow sediment layer thickness between 300–760 m with an average of 460 m. These variations in sediment thickness indicate that topographic conditions, geological structures, and the development of local tectonic and volcanic features strongly influence the sediment depth profile in each area.

Several previous studies in geothermal and tectonic areas generally used gravity methods to determine sediment thickness from the depth of residual anomalies, using field data and GGMPlus satellite data, which are relatively accurate. Similar studies based on TOPEX satellite gravity data remain limited, primarily because of its low spatial resolution, high noise in coastal areas, and greater interpretation uncertainty compared to field gravity surveys. TOPEX's relatively coarse resolution results in poorly defined small-scale anomalies and shallow structures, making this method more effective for regional analysis. Nevertheless, TOPEX has advantages for mapping subsurface conditions; thus, it was selected as the data source in this study. The limited data accuracy in this study underscores the need for further research development through multi-satellite integration and field validation to improve the reliability of geophysical interpretations.

4.5. SVD Anomaly

The Second Vertical Derivative (SVD) map of gravity anomaly data is a second-order vertical derivative that highlights shallow gravity anomalies (Blakely, 1996; Elkins, 1951). This map is very effective for identifying geological structure boundaries, such as faults,

sedimentary basin edges, and lithological contacts, because it clarifies lateral changes in rock density (Siombone et al., 2021, 2022). The SVD data are derived from residual Bouguer anomalies using the SVD filter operator (Siombone et al., 2021, 2022). The SVD map is shown in **Figure 10**.

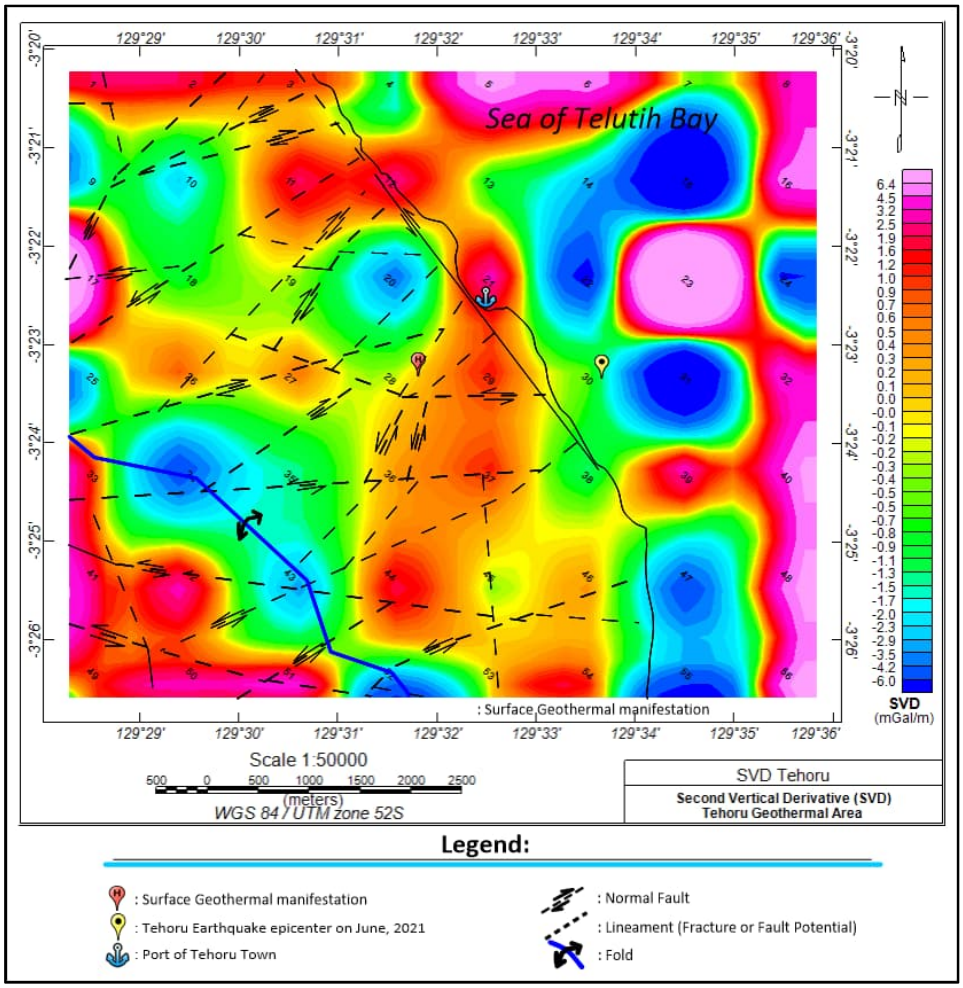

Figure 10. SVD Map with Geological features of the Study Area.

Based on **Figure 10**, the SVD anomaly in the study area ranges from -6.10 mGal/km² to 6.30 mGal/km². This SVD anomaly map is very helpful for highlighting the contact boundaries of geological structures in the study area, including faults, lineaments, and folds. The interpretation is strengthened when the SVD anomaly map is overlaid with the local geological structure map of the study area. Based on the SVD map overlaid with local geological structure data (**Figure 10**), geothermal manifestations on the surface, such as hot springs and steaming soil, tend to occur in areas flanked by several normal fault lines. These results are in line with Siombone (2022) research, which found that surface manifestations, such as hot springs and steaming soil, in the geothermal area of Tehoru Village tend to occur in areas with high lineament density. The lineaments in question can be faults and fractures (Ilham et al., 2025; Siombone et al., 2022). The orientation of the lineament and fault structure patterns in the Tehoru geothermal area, as shown by the geological structure overlay on the SVD map in **Figure 10**, is further supported by interpretations of the ridge-and-valley lineaments and Rose diagram analyses in **Figures 11** and **Figure 12**.

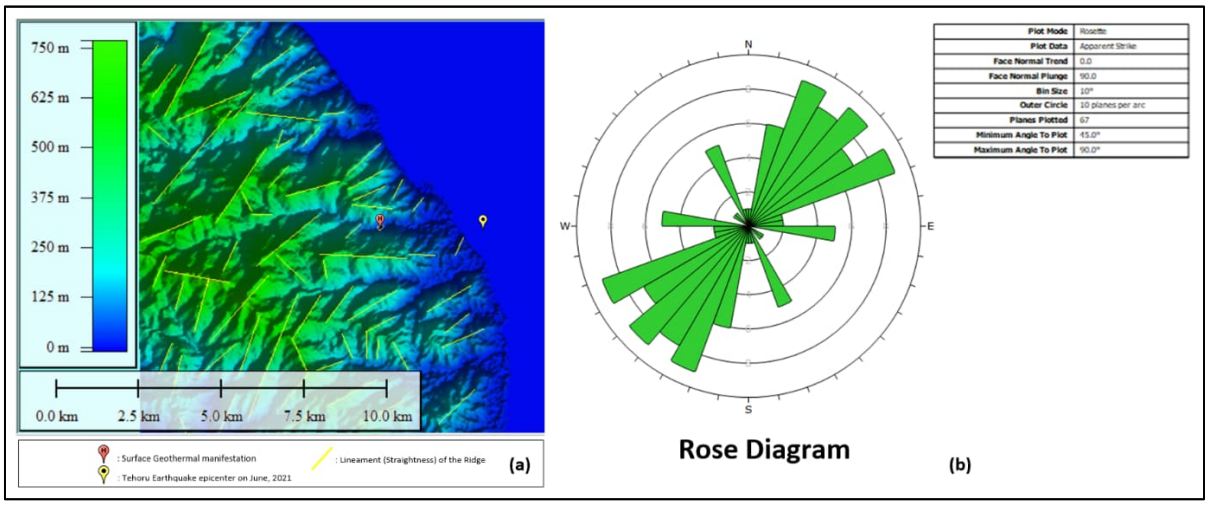

Figure 11. (a) Ridge Lineament, and (b) Rose diagram of ridge lineament with Azimuth 135°.

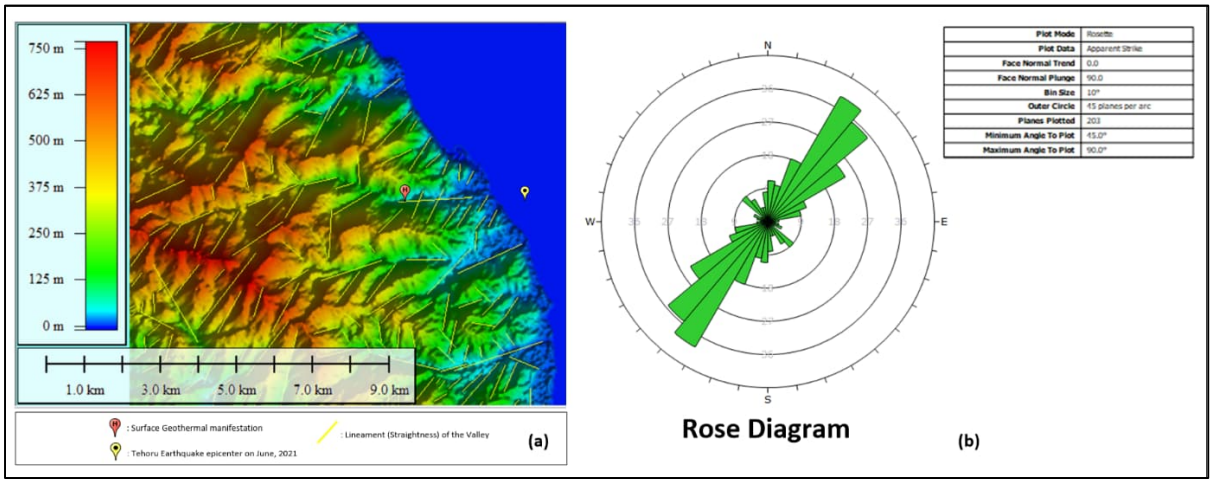

Figure 12. (a) Valley Lineament, and (b) Rose diagram of valley lineament with Azimuth 135°.

Figure 11a and **Figure 12b** are ridge lineament maps and valley lineament maps that were manually digitized by utilizing SRTM DEM data in the Global Mapper app v.19 application, by utilizing the digitizer tool feature for the "create line feature" option. After the lineament data were collected, they were exported as a CSV file, which was then imported into the Dips 7.0 application by selecting the global-oriented format "STIKE/DIPR" to be visualized as a rose diagram in **Figures 11b** and **Figure12b**. Based on **Figure 11a**, a ridge lineament map shows that the lineaments are arranged following a ridge lineament pattern with an azimuth of 135°. The visual analysis of the map identified 67 ridge lineaments. Furthermore, the Rose diagram in **Figure 11b** shows that the ridge lineaments form a dominant structural orientation with a Southwest–Northeast direction. Based on **Figure 12a**, a valley lineament map shows that the lineaments are built following the valley lineament pattern in the hill morphology, with an azimuth angle of 135°. Visual analysis of the map identified 203 valley lineaments. The Rose diagram in **Figure 12b** shows that the valley lineaments have a dominant structural orientation toward Southwest–Northeast, consistent with the ridge lineament orientation pattern in **Figure 11b**.

Analysis of the SVD anomaly map in **Figure 10** shows the presence of a west-east-oriented normal fault that connects the geothermal prospect area to the epicenter of the Tehoru earthquake on June 6, 2021. Overlaying local

geological structures indicates the existence of several local faults and lineament in arround Tehoru Village, predominantly oriented southwest-northeast. The complexity of the fault structure can increase earthquake shaking intensity through ground deformation and liquefaction (Yanis et al., 2025). In addition to structural factors, sediment thickness, as shown in **Figures 9a** and **Figure 9b**, also contributes to seismic wave amplification and structural damage during earthquakes (Maringue et al., 2021; Safitri et al., 2023; Setianegara et al., 2023).

5. CONCLUSION

Based on TOPEX gravity data processing, the Tehoru geothermal area shows a Complete Bouguer Anomaly (CBA) value of 6.80–73.60 mGal with a dominance of low anomalies in the western part. The reduced-Bouguer density values from the Parasnis method (ρ = 1.79 g/cm^3) and the Nettleton method (ρ = 1.77 g/cm^3) indicate the dominance of alluvial sediments. Residual anomalies range from -4.60 to 47.70 mGal, with a distribution pattern following a high-density fault zone, while 3D modeling shows an average sediment thickness of ±246.07 m. SVD, lineament, and rose diagram analyses confirm that geothermal manifestations are controlled by a fault system and lineament alignments oriented northeast–southwest. The combination of active structures and thick sediments indicates the potential for seismic-wave amplification (site amplification) in the Tehoru area. Therefore, the integration of complementary geophysical methods, including magnetic, seismic, geoelectrical, magnetotelluric, and high-resolution satellite gravity techniques, is recommended to improve the accuracy of subsurface models and enhance the characterization of the Tehoru geothermal system.

ACKNOWLEDGMENT

The authors would like to thank NASA (National Aeronautics and Space Administration) and CNES (Centre national d'études spatiales) for providing TOPEX/Poseidon satellite data in the form of global gravity and topography data. Thanks are also extended to NASA and NGA (National Geospatial-Intelligence Agency, United States) for providing DEM data from the Shuttle Radar Topography Mission (SRTM), which played a crucial role in supporting this research.

REFERENCES

Abdelrahman, E. M. & El-Araby, T. M. (1996). Shape and Depth Solutions From Moving Average Residual Gravity Anomalies. *Journal of Applied Geophysics*, Vol. 36.

Abdullahi, M. (2022). *Gravity Anomaly and Basement Estimation Using Spectral Analysis*. https://doi.org/10.5772/intechopen.99536

Andayany, H. & Risakotta, M. Y. S. (2017). Application of Geotermometry Equation (SiO2)p in The Geothermal Areas Both Haruku and Tehoru, Central of Maluku. *International Journal of Health Medicine and Current Research*, *2*(04), 605–609. https://doi.org/10.22301/IJHMCR.2528-3189.605

Armi, R. (2025). Spectral Analysis in the Separation of Gravity Anomalies: Implications for Disaster Risk Reduction in the West Coast of Aceh. *Earth Sciences Research Journal*, *29*(4), 399–407. https://doi.org/10.15446/esrj.v29n4.116923

Blakely, R. J. (1996). *Potential Theory in Gravity and Magnetic Applications* (1st ed., Vol. 1). Cambridge University Press. https://doi.org/https://www.eoas.ubc.ca/academics/courses/eosc450/ewExternalFiles/Blakely_PotentialFieldsText.pdf

Daniarsyad, G., Priyobudi, P., Cahyaningrum, A. P., Wibisono, D. G., Sriyanto, S. P. D., Rosid, A., Pranata, B., Gunawan, I., Fatchurochman, I., & Daryono, D. (2023). Analysis on the Causative Fault of the 2021 Mw 6.0 Tehoru Earthquake in the South Coast of Seram Island: A Preliminary Result. *E3S Web of Conferences*, *447*. https://doi.org/10.1051/e3sconf/202344701020

Dewanto, B. G., Margiono, R., Segoro, Y. A., Pramesthi, E., & Maimuna, A. K. (2023). The Importance of Gravity Data For Estimating and Identifying The Sediment Thickness of Subsurface Structure Around Majene Sulawesi Barat. *AIP Conference Proceedings*, *2654*. https://doi.org/10.1063/5.0115361

Directorate of Geothermal Energy (2017). *Potential Geothermal Indonesia Vol. 1* (1st ed., Vol. 2). Directorate General of New, Renewable Energy and Energy Conservation, Ministry of Energy

and Mineral Resources. https://www.esdm.go.id/en/berita-unit/directorate-general-ebtke/peluncuran-buku-potensi-panas-bumi-indonesia-2017

Elkins, T. A. (1951). *The Second Derivative Method of Gravity Interpretation*. *06*(1), 29–50. https://doi.org/10.1190/1.1437648

Gunawan, H., & Mikhailov, V. (2008). Estimation of Bouguer Density Precision: Development of Method for Analysis of La Soufriere Volcano Gravity Data. *Jurnal Geologi Indonesia* (Vol. 3, Number 3).

Hill, K. C. (2012). Tectonic and Regional Structure of Seram and the Banda Arc. *Indonesian Journal of Sedimentary Geology*, *23*(1), 5–61. https://doi.org/https://doi.org/10.51835/bsed.2012.23.1.187

Ilham, Susilo, A., Sukanta, I. N., Siregar, D. V., Hasan, M. F. R., & Hardianto, Y. P. (2025). Detecting Active Fault with the Topographic Gravity Model: A Case Study from Turen, Indonesia. *Iraqi Geological Journal*, *58*(2), 203–215. https://doi.org/10.46717/igj.2025.58.2A.13

Maringue, J., Sáez, E., & Yañez, G. (2021). An Empirical Correlation Between The Residual Gravity Anomaly and The H/V Predominant Period in Urban Areas and Its Dependence on Geology in Andean Forearc Basins. *Applied Sciences (Switzerland)*, *11*(20). https://doi.org/10.3390/app11209462

Nettleton, L.L. (1939). Determination of Density For Reduction of Gravimeter Observations. *Geophysics*, *4*(3), 176–183. https://doi.org/https://doi.org/10.1190/1.1437088

Pelupessy, W. V., & Silverman, R. M. (2024). Exploring Indonesian Coastal Communities' Responses To The 2019 Ambon Earthquake and Preparedness For Future Disasters. *International Journal of Disaster Risk Reduction*, *114*. https://doi.org/10.1016/j.ijdrr.2024.104961

Peng, W., Cheng, T., Wang, S., Zhao, H., Pang, L., Zhou, X., Wang, J., & Chen, Z. (2025). Basement Depth Estimation of The Red Sea Basin From Gravity Data and Drilling Data. *Journal of Geophysics and Engineering*, *22*(4), 963–970. https://doi.org/10.1093/jge/ gxaf046

Prabowo, U.N., Raharjo, S.A., & Ariska, L. (2022). *Power Spectrum Analysis of the Satellite Gravity Anomalies Data to Estimate the Thickness of Sediment Deposits in the Purwokerto-Purbalingga Groundwater Basin*. http://topex.ucsd.edu/cgi-bin/get_data.cgi,

Prasetyo, I., Kadir, W. G. A., Abdurrahman, D., Dahrin, D., Ibrahim, K., & Kurniawan, A. (2025). New Insight into the Structural Model in Southern Sumatra Indonesia using Gravity and Magnetic Data: Implications for Geothermal Resources. *Rudarsko Geolosko Naftni Zbornik*, *40*(2), 43–60. https://doi.org/10.17794/rgn.2025.2.4

Ramadhan, I., & Pohan, A. F. (2024). Pemisahan Anomali Regional dan Residual pada Metode Gravitasi Menggunakan Metode Moving Average, Upward Continuation dan Polynomial. *Jurnal Fisika Unand*, *13*(1), 1–7. https://doi.org/10.25077/jfu.13.1.1-7.2024

Rasimeng, S., Dani, I., Syahranti, W. P., Sitompul, I. J., & Nizam, F. M. (2024). Identification of Regional Rock Depth-Residual Gravity Anomaly Based on Spectrum Analysis of Geothermal Prospect Area of Way Ratai Lampung. *Gravity : Jurnal Ilmiah Penelitian Dan Pembelajaran Fisika*, *10*(1). https://doi.org/10.30870/gravity.v10i1.23575

Safitri, A. N., Sarwanto, S., & Harjunowibowo, D. (2023). Pengembangan Modul Pembelajaran Fisika Berbasis Kearifan Lokal Pada Materi Suhu dan Kalor. *Jurnal Materi Dan Pembelajaran Fisika*, *13*(1), 32. https://doi.org/10.20961/jmpf.v13i1.60093

Samalehu, H., Idrus, A., & Nugroho Imam Setiawan. (2024). Geology of Tamilouw-Haya, Tehoru District, Central Maluku Regency, Maluku Province. *Jurnal Geologi dan Sumberdaya Mineral-Terakreditasi KEMENRISTEKDIKTI*, *23*(3), 177–187. https://doi.org/10.33332/jgsm.geologi.v23.3.177-187

Sandwell, D. T., Müller, R. D., Smith, W. H. F., Garcia, E., & Francis, R. (2014). New Global Marine Gravity Model From CryoSat-2 and Jason-1 Reveals Buried Tectonic Structure. *Science*, *346*(6205), 65–67. https://doi.org/10.1126/science.1258213

Sapiie, B., & Hadiana, M. (2013). Analogue Modeling of Oblique Convergent Strike-Slip Faulting and Application to The Seram Island, Eastern Indonesia. In *Indonesian Journal on Geoscience* (Vol. 1, Number 3).

Sarkowi, M. (2014). *Gravity Exploration* (1st ed., Vol. 1). Graha Ilmu.

Segoro, Y. A., & Margiono, R. (2025). Identification Sub-Surface Structure and Sediment Depth Estimation at the Proposed Indonesian New Capital City. *Indonesian Journal of Applied*

Physics, *15*(2), 409. https://doi.org/10.13057/ijap.v15i2.96059

Setianegara, R., Muslim, D., Ismawan, & Marjiyono (2023). Potensi Penguatan Gelombang Gempabumi oleh Sedimen Permukaan Berdasarkan Analisis Mikrotremor: Studi Kasus di Cekungan Bandung Bagian Selatan. *Jurnal Geologi Dan Sumberdaya Mineral*, *24*(2), 107–115. https://doi.org/10.33332/jgsm.geologi.v24i2.749

Sfada, S. A. & Ali, A. (2025). Gravity Based Mapping of Sedimentary Thickness And Structural Trends in The Sokoto Basin, Northwestern Nigeria. *Geological Behavior*, *9*(1), 01–07. https://doi.org/10.26480/gbr.01.2025.46.52

Siombone, S.H. (2022). Analisis Suhu Permukaan dan Kondisi Geomorfologi Kawasan Geotermal Tehoru Menggunakan Landsat-8 dan DEM. *JGE (Jurnal Geofisika Eksplorasi)*, *8*(3), 210–224. https://doi.org/10.23960/jge.v8i3.243

Siombone, S. H., Lestari, F. A., & Wiyono. (2024). Contextual Physics Learning Based on Geothermal Areas to Improve Scientific Literacy and Scientific Communication Skills. *Jurnal Pendidikan MIPA*, *25*(2), 986–1011. https://doi.org/10.23960/jpmipa/v25i2.pp986-1011

Siombone, S. H., Susilo, A., & Maryanto, S. (2022). Integration of Topex Satellite Gravity and DEM SRTM Imagery for Subsurface Structure Identification at Tiris Geothermal Area, Lamongan Volcano Complex, Probolinggo, East Java. *POSITRON*, *12*(2), 98. https://doi.org/10.26418/positron.v12i2.56880

Sismanto, Hoerunisa, A., Risdianto, D., & Rahadinata, T. (2022). The Investigation of Kadidia Geothermal Field (Indonesia) Using Gravitational Data and Power Spectrum Analysis. *Jurnal Teknologi*, *84*(1), 149–157. https://doi.org/10.11113/jurnalteknologi.v84.17489

Toisuta, Y. M. K., Haryanto, A. D., Hutabarat, J., & Gentana, D. (2021). Pendugaan Temperatur Bawah Permukaan pada Manifestasi Panas Bumi Berdasarkan Analisis Geokimia Air Panas Daerah Kecamatan Tehoru, Kabupaten Maluku Tengah, Provinsi Maluku. *Geoscience Journal, 5*, 267–279. https://journals.unpad.ac.id/geoscience/article/view/35231

Tjokrosapoetro, A. S, Achdan, E. Rusmana, & H.Z. Abidin. (1993). *Geology of ke Masohi Quadrangle, Maluku* (Surono & T.O. Simanjuntak, Eds.; 1st ed., Vol. 1, pp. 1–17). Geological Research and Development Center, Indonesia.

USGS (2016). *Landsat 8 (L8) Data Users Handbook* (2.0, Vol. 8, pp. iii–76). EROS, Department of the Interior U.S. Geological Survey. https://www.usgs.gov/media/files/landsat-8-9-olitirs-collection-2-level-2-data-format-control-book

Wahyudi, E. J., Santoso, D., & Ahmad Firdaus, M. U. (2019). Gravity Survey in Pandan Mountain - East Java, Indonesia. *Journal of Physics: Conference Series*, *1204*(1). https://doi.org/10.1088/1742-6596/1204/1/012006

Yanis, M., Ananda, R., Adhari, M. R., Paembonan, A. Y., & Ghani, A. A. (2025). Mapping The Geological Fault Zone That Triggered The Mw 6.1 Pasaman Earthquake in Indonesia on The Basis of Gravity Anomalies. *Geologos*, *31*(2), 151–166. https://doi.org/10.14746/logos.2025.31.2.12

Zakariah, M. N. A., Roslan, N., Sulaiman, N., Lee, S. C. H., Hamzah, U., Noh, K. A. M., & Lestari, W. (2021). Gravity Analysis For Subsurface Characterization and Depth Estimation of Muda River Basin, Kedah, Peninsular Malaysia. *Applied Sciences (Switzerland)*, *11*(14). https://doi.org/10.3390/app11146363